J. Physiol. (1976), **262**, *pp.* 285–300
With 6 text-figures
Printed in Great Britain

CURRENT–VOLTAGE RELATIONSHIPS IN THE CRYSTALLINE LENS

BY ROBERT S. EISENBERG AND JAMES L. RAE

From the Department of Physiology, University of California, Los Angeles, California, and Departments of Ophthalmology and Physiology and Biophysics, University of Texas Medical Branch, Galveston, Texas, U.S.A.

(*Received 20 January 1976*)

SUMMARY

1. Electrical coupling between the cells of the crystalline lens of the frog eye was studied using two intralenticular micro-electrodes, one to pass current and one to record potential. In most experiments, both electrodes were placed just inside the posterior surface of the lens at a depth of approximately 200 μm from the surface. Step functions of current were applied and the time course of the resulting change in voltage was measured at many different electrode separations.

2. The voltage change has both a fast component, which occurs only locally in the region close to the current passing micro-electrode, and a slow component, which is spatially uniform, independent of distance from the current micro-electrode.

3. This behaviour is predicted by an electrical model of a single large spherical cell, and so that model can be used to analyse our data.

4. The resistivity of the lens 'interior' (both cytoplasm and coupling resistivity) is 625 Ω cm; the resistance of the lens 'membrane' is 2751 Ω cm^2.

5. The data and analysis help to reconcile discrepancies between previous measurements of the electrical properties of the lens and show clearly that there is substantial electrical coupling from cell to cell. The method should allow investigation of the role of electrical coupling in cataract formation in the crystalline lens.

INTRODUCTION

The crystalline lens of the eye is an almost spherical, transparent structure containing two kinds of cells. The first forms a single layer of almost cuboidal epithelial cells on the anterior side only. The second is a fibre cell, formed at the lens equator, which grows into an exceptionally long cell extending from almost the mid-anterior side of the lens all the way around

to almost the mid-posterior side. As new fibre cells are formed, the old cells are pushed in toward the centre of the lens, which results in many of these U-shaped fibres being piled on top of each other in columns. The cells are very tightly packed both within columns and between columns. The entire lens is surrounded by a tough collagenous capsule.

Brindley (1956) discovered that the inside of the lens maintained a substantial negative (−75 mV) potential difference (p.d.) with respect to its bathing medium. The p.d. was highly susceptible to localized damage. Andree (1958) later reported that microdissection of only the outermost layers of lens cells caused a reduction in the potential difference of the entire lens as though the cells deeper might not be maintaining a potential difference across their membranes.

Duncan (1969) made micro-electrode resistance measurements within the intact lens of the toad. Two relatively large tipped (3–5 μm) micro-electrodes were inserted into the lens, and currents in the microamp range were passed between one of them and a large electrode in the bath. A potential difference was recorded differentially between the other micro-electrode and a similar micro-electrode in the bath. Duncan was able to measure such an induced potential difference for all separations of the intralenticular current and voltage micro-electrodes. He further reported that this induced potential was the same for all separations of the electrodes. The induced voltage had a long time constant, taking about a second or so after the onset of an approximately 2 sec current pulse to reach its maximal value. On the basis of these 'input resistance' findings and other data, he concluded that the membranes of the cells below the surface of the lens were 'degenerate'; later (Duncan, 1973) he described the cells as 'electrically coupled'.

Rae & Blankenship (1973) reported input resistances from the frog lens measured with double-barrelled micro-electrodes, i.e. two micro-electrodes cemented together, with tips a fraction of a micron apart. They found input resistances of 1–6 MΩ within any one lens in comparison to the approximately 5 kΩ values reported by Duncan. In addition, the induced voltage had a short time constant and reached a steady state in less than 20 msec. A long time constant component was not seen. The authors tentatively concluded that they were charging single lens fibres.

Both of these previous studies failed to consider adequately the spatial spread of the induced potential. When current is injected from a micro-electrode, the potential in the immediate vicinity is very large. The micro-electrode is essentially a point source and the small dimension of the conductor near the point source ensures that the effective resistance (often called convergence resistance) of the conducting material near the micro-electrode is very high. This large potential is confined to the region in the

immediate vicinity of the micro-electrode. Away from the micro-electrode, the dominant resistance to current flow (from the micro-electrode to an external electrode in the bathing medium) is the membrane, the internal resistance being essentially negligible. Thus, the potential away from the micro-electrode source is dominated by the membrane resistance and is essentially independent of location. Recent publications have analysed three dimensional 'cable' theory of spherical cells (Barcilon, Cole & Eisenberg, 1971; Eisenberg & Engel, 1970; Eisenberg & Johnson, 1970; Peskoff & Eisenberg, 1973; Peskoff & Eisenberg, 1975), have described the spatial spread of potential, and have shown that the local potential near the current micro-electrode is quickly established (essentially instantaneously on the physiological time scale), whereas the potential a long distance from the electrode grows more slowly on the usual physiological time scale of milliseconds–seconds. It would seem attractive to apply that analysis to the current–voltage relationship in the crystalline lens since the lens is roughly spherical in shape and evidence exists that internal lens cells are closely coupled (Duncan, 1969, 1973; Rae, 1974*a*, *b*).

In the spherical cell analysis of Peskoff & Eisenberg (1975) the induced potential produced by a step function of current for a cell in an infinite bath with a remote current sink is described as follows:

$$
\begin{aligned}
V = {} & \frac{IR_{\mathrm{m}}}{4\pi a^2}(1-\exp(-t/R_{\mathrm{m}}C_{\mathrm{m}}))+\frac{IR_{\mathrm{i}}}{4\pi a}\left\{\left(\frac{r_1^2+R_1^2}{a^2}\right)-\frac{2r_1R_1}{a^2}\cos\theta\right\}^{-\frac{1}{2}} \\
& +\frac{IR_{\mathrm{i}}}{4\pi a}\left\{\left(1+\frac{r_1^2R_1^2}{a^4}-\frac{2r_1R_1}{a^2}\cos\theta\right)^{-\frac{1}{2}}-2+\log_{\mathrm{e}}2\right\} \\
& -\frac{IR_{\mathrm{i}}}{4\pi a}\log_{\mathrm{e}}\left\{1-\frac{r_1R_1}{a^2}\cos\theta+\left(1+\frac{r_1^2R_1^2}{a^4}-\frac{2r_1R_1}{a^2}\cos\theta\right)^{\frac{1}{2}}\right\} \\
& +\frac{IR_{\mathrm{b}}}{4\pi a}, \qquad (1)
\end{aligned}
$$

where

V = potential (V),

I = current applied (A),

a = radius of cell (cm),

t = time after onset of current step (sec),

C_{m} = membrane capacitance (F/cm^2),

R_{i} = internal resistivity (Ω cm),

R_{m} = membrane resistance ($\Omega\ \mathrm{cm}^2$),

R_1 = radial location of current electrode (cm) = distance from centre of cell,

r_1 = radial location of voltage electrode (cm) = distance from centre of cell,

θ = angular separation of electrode tips,

R_b = resistivity of bathing solution ($\approx$ 80 Ω cm).

Note that in the experiments reported here, $R_1 \simeq r_1 \simeq a$. Note also that the term $IR_b/4\pi a$ is later shown to be negligible.

For the purpose of the present study, the most relevant predictions of the equation are as follows.

(1) When a rectangular-current pulse is passed between an intracellular electrode and an external bath electrode located far from the cell, the time course of the induced potential has two components. One is a very fast component which has the same time course as the current pulse. This is a local potential which dies away a small distance from the current micro-electrode. The second is a slower component which is independent of distance from the current micro-electrode.

(2) The slow component depends upon R_m, but not at all upon R_i. It is determined by term 1 of eqn. (1).

(3) The fast component depends upon R_i and R_b, but not at all upon R_m. It is determined by terms 2, 3, 4 and 5 of eqn. (1). While the fast component of the potential is described in (1) as if it is instantaneous, Peskoff & Eisenberg (1975) have analysed its time course and have shown it to be very fast, but not instantaneous.

It is the purpose of this paper to report recent findings on current–voltage relationships in the crystalline lens of the frog, obtained using an intralenticular two micro-electrode technique, and to analyse these relationships using the theoretical analysis summarized in eqn. (1).

We expect the circuit of the lens to be complex. For example, we know that the slow component can be split into at least two spatially independent components. However, since we are interested in the over-all resistive and total capacitative properties of the lens, we choose to consider a single, composite slow component.

METHODS

All experiments were done on 2½–3 in grass frogs (*Rana pipiens*) with lenses whose equatorial diameters were about 0·4 cm. The dissection procedures and physiologic saline solution used have been described elsewhere (Rae, 1973). The lenses were not perfectly spherical. Rather, their dimensional ratio was as follows:

$$\frac{\text{anterior} - \text{posterior}}{\text{equatorial}} \approx 0{\cdot}89.$$

All measurements were made on the posterior surface of the lens since the thinner capsule located there was more easily penetrated with micro-electrodes than was the thicker anterior capsule. The voltage between the inside of the lens and the bath

was measured differentially using matched 5–7 MΩ, 3 M-KCl-filled micro-electrodes and a W. P. Instruments Model 750 dual microprobe electrometer (Hamden, Conn.). One electrode was placed within the lens using a David Kopf (Tujunga, Ca.) stepping motor-driven hydraulic micromanipulator, the other in the bath about 0·5 mm from the lens surface. The location of the bath electrode was unimportant since the extracellular potential was always negligible (see below). Only lenses having an initial 'resting potential' between −70 and −75 mV were used for the studies. If the 'resting potential' changed by more than 5 mV during the course of an experiment, the data from the experiment were discarded. Current was passed through a micro-electrode with a tip diameter of about 1 μm which was filled with 2 M potassium citrate titrated to neutrality with citric acid. The Ag–AgCl pellet-electrode current sink was located in the bath at a distance of at least 7 lens diameters from the lens. The current micro-electrode was surrounded with a grounded aluminium foil shield to reduce capacitative transients in the potential recording and was placed in the lens using a Prior (Eric Sobatka, Sarasota, Fla.) micro-manipulator. Constant current was supplied from a locally constructed current clamp utilizing a Datel (Canton, Mass.) Model Am 3018 high-voltage op-amp in a Howland current pump circuit (Philbrick Researchers, 1966). Care was taken in the construction of this circuit to ensure that the circuit was capable of delivering 1·2 μA of constant current with a time constant of 300 μsec through at least 10 MΩ.

The lateral separation of the current and voltage electrodes was determined either with an eyepiece micrometer and a Wild M 5 dissecting microscope or by measuring the tip separation in photographs taken through the dissecting microscope. The error in measurement is approximately 0·6° (≈ 20 μm) and contributes seriously to the scatter of our experimental data (Figs. 5, 6).

The electrodes were inserted just below the surface of the lens. The depth of the micro-electrodes in the lens was determined either directly from the calibrated micrometer screw on the Prior micromanipulator or by counting the number of pulses activating the 1 μm/step stepping motor of the David Kopf micromanipulator. When the micro-electrode tip first touched the lens surface a 1–5 mV potential change always occurred. The micromanipulator position at which this change occurred was defined as reference depth zero. The angular separation of the electrodes could be determined from the measured depth, lens radius, and lateral separation using trigonometric formulae.

The potential, after suitable amplification, was fed into the sample and hold amplifiers of A–D converters connected to a Digital Equipment Corporation (Maynard, Mass.) PDP 8/E computer and the data was processed using Daquan, a programme supplied by Digital Equipment Corporation. This programme allowed averaging, slope correction for a drifting base line, digital filtering, oscilloscope display, and plots on an analogue x–y plotter. Two records were collected for each separation of the electrodes. The first was an average of five responses, each for 15 sec, to 8 sec current pulses. This average was used to establish the amplitude of the sum of the fast and slow components. The second record was an average of 100 responses, each for 80 msec, to 100 msec current pulses. This average, both filtered and unfiltered, was used to establish the amplitude of the fast component.

Induced potential and electrode angular separation data were punched on paper tape and fed into a Digital Equipment Corporation Model 11/40 computer for curve fitting analysis. The programme (Dixon, 1974) utilizing a least-squares method, allowed R_m and R_i to float while holding a, t, R_1, r_1, C_m and R_b constant for specified values of V and θ. Best fit values for R_m and R_i were returned along with goodness of fit statistics.

RESULTS

Fig. 1 shows a typical induced potential measured at an electrode separation of 30 μm during a 500 nA, 8 sec current pulse. It can readily be seen that the response has two components. One is a fast component (a) which appears as an instantaneous voltage step on this time scale and the

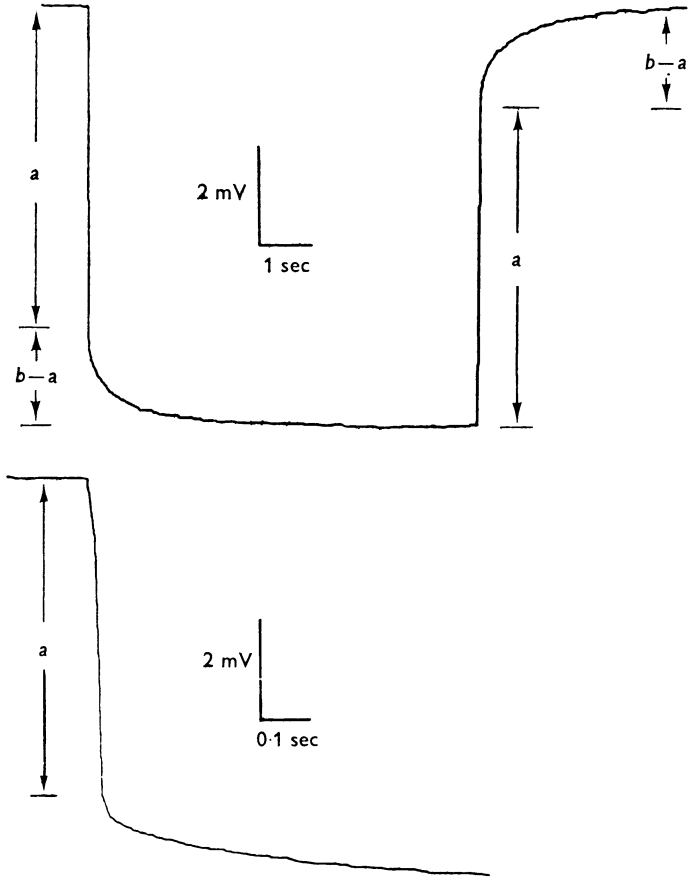

Fig. 1. Typical x–y plot of induced voltage response to a 500 nA square current pulse on two different time scales. Electrode angular separation is 1°. Both electrodes are placed just under the lens surface. Response contains a fast component (a) and a slow component ($b-a$).

second is a slow component ($b-a$) which takes 3–4 sec to reach its maximum amplitude. The voltage response can be analysed only if it can be verified that the current pulses are not disrupting the normal lens tissue. Possible tissue disruption was initially a matter of some concern since

lines of optical discontinuity oriented along the long axis of the lens fibres could be seen through the dissecting microscope in the region adjacent to the tip of the current electrode. Such 'structural alteration' was seen to disappear completely 5–10 min after cessation of current pulses. Histologic sections through the region in question showed no obvious structural alteration at the light-microscopic level. The question of structural damage was investigated further by establishing voltage–current relationships at various positions in a few lenses. A typical result

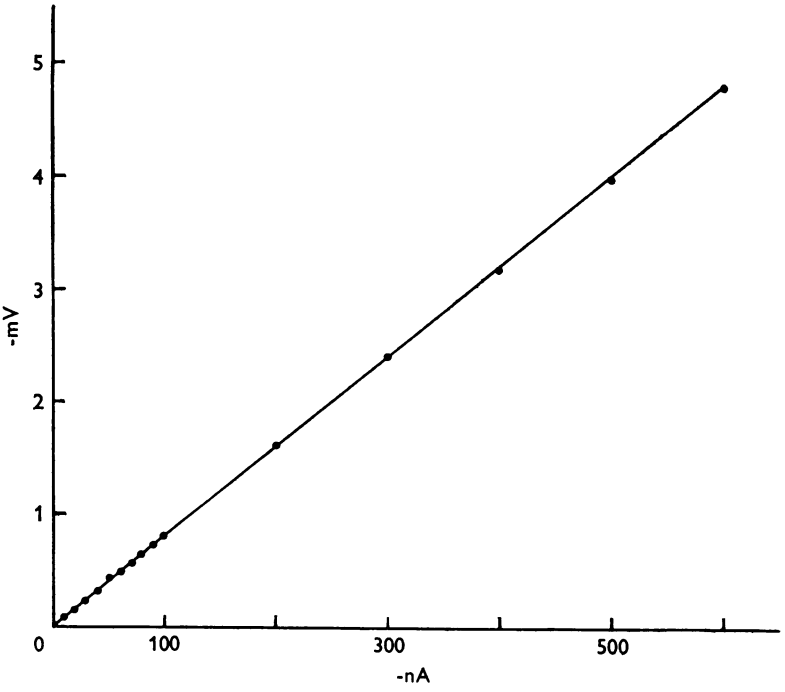

Fig. 2. Typical plot of hyperpolarizing induced voltage responses as a function of the magnitude of the square current pulses. Electrode angular separation is approximately 10°. Both electrodes are placed just under the lens surface.

is shown in Fig. 2. Low currents (10 nA) were used initially followed by increasingly larger currents. It was reasoned that, if structural damage was occurring, the slope of the curve should change after repeated measurements at higher current levels. All such experiments resulted in very linear relationships as depicted in Fig. 2. A few experiments were also done where the voltage response to a 10–25 nA current pulse was recorded. The current was then increased to 1·2 μA for several minutes followed by another recording of the response to a 10–25 nA current pulse. In each

case, the second response to low currents was virtually identical to the first, again suggesting that no appreciable tissue damage was occurring.

To test the predicted isopotentiality of the slow component and the predicted steep spatial decrement of the fast component, it was necessary to ensure that we could adequately separate the two components from our measured responses. Utilizing the computer averaging techniques previously described, we were able to construct plots as shown in Fig. 3.

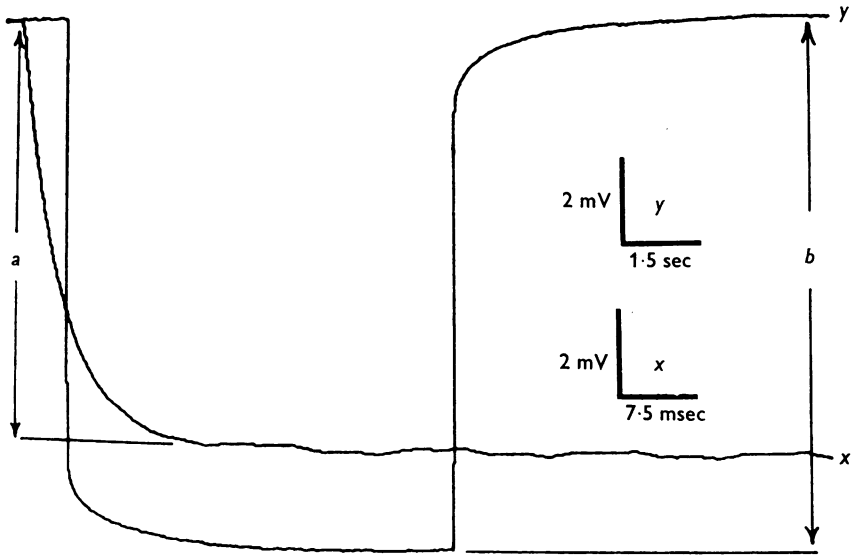

Fig. 3. Typical x–y plot of computer separation of fast component from total induced response. Curve y is average of five responses for 15 to 8 sec 500 nA current pulses. Curve x is average of 100 responses for 80 msec to 100 msec 500 nA current pulses. Amplitude of fast component is a, amplitude of total response is b. Electrode angular separation is approximately 0·8°. Both electrodes are placed just under the lens surface.

Curve x is the average of 100 responses to 100 msec, 500 nA pulses for a fixed electrode separation shown on a fast time base. The gradually sloping slow component is extrapolated to $t = 0$. The amplitude (a) of the fast component is the voltage at which this extrapolated line crosses $t = 0$. The frequency response of the amplifier was limited (-3 dB at 500 Hz) to suppress a rapid capacitative transient which otherwise would be apparent in these fast component averages. However, it was verified that the fast component measured in this manner is independent of the band width of the amplifier. Curve y is the average of five responses to 8 sec, 500 nA pulses for the same electrode separation as in curve x. The amplitude of the slow component was the difference ($b-a$) between the

total response (*b*) and the fast component (*a*). Averages taken with all electrodes in the bath, or with both potential electrodes in the bath and the current electrode in the lens, showed no slow component even when it was possible to place the recording electrode close enough to the current source to show a fast component.

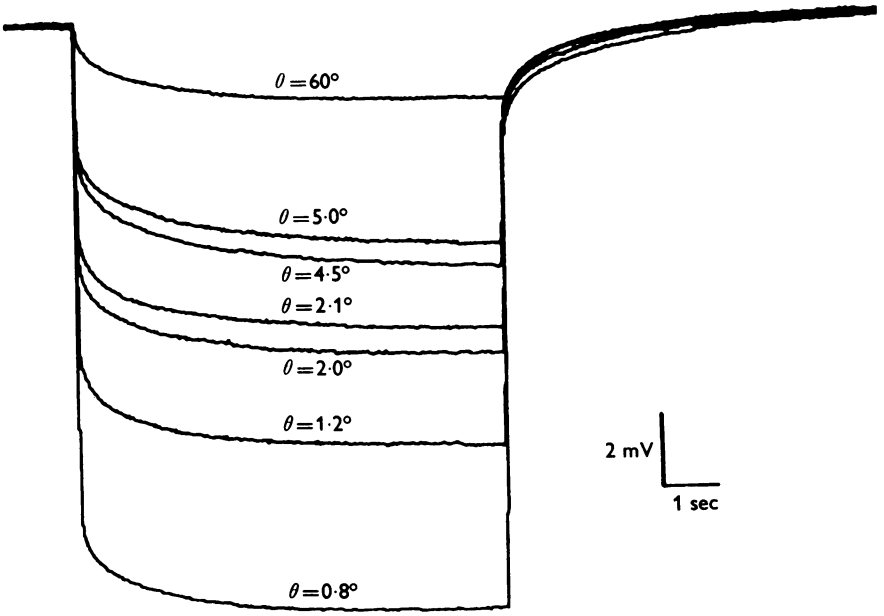

Fig. 4. Superimposed x–y plots of seven induced voltage responses for varying electrode angular separations in same lens. Numbers (θ) represent degrees of electrode separation. Both electrodes are placed just under lens surface. Current pulses are 500 nA for 8 sec.

Multiple superimposed responses to 8 sec, 500 nA pulses for varying electrode separations in the same lens (Fig. 4) show qualitatively the results predicted by the theoretical equation. That is, as the electrodes are moved farther and farther apart, the fast component disappears, whereas the slow component is relatively unchanged. The similar time course of each slow component should also be noted. Five of the seven responses shown follow the same decay time course and the other two show only small deviations from it. Those deviations probably result from the DC drifts which can occur during the measurements.

Data from two typical experiments are shown in Fig. 5 (*A*, *B*). In each of these, the total induced amplitude (*b*), the amplitude of the fast component (*a*), and the amplitude of the slow component ($b-a$) are plotted as a function of the angular separation of the electrodes (θ). Again, it can

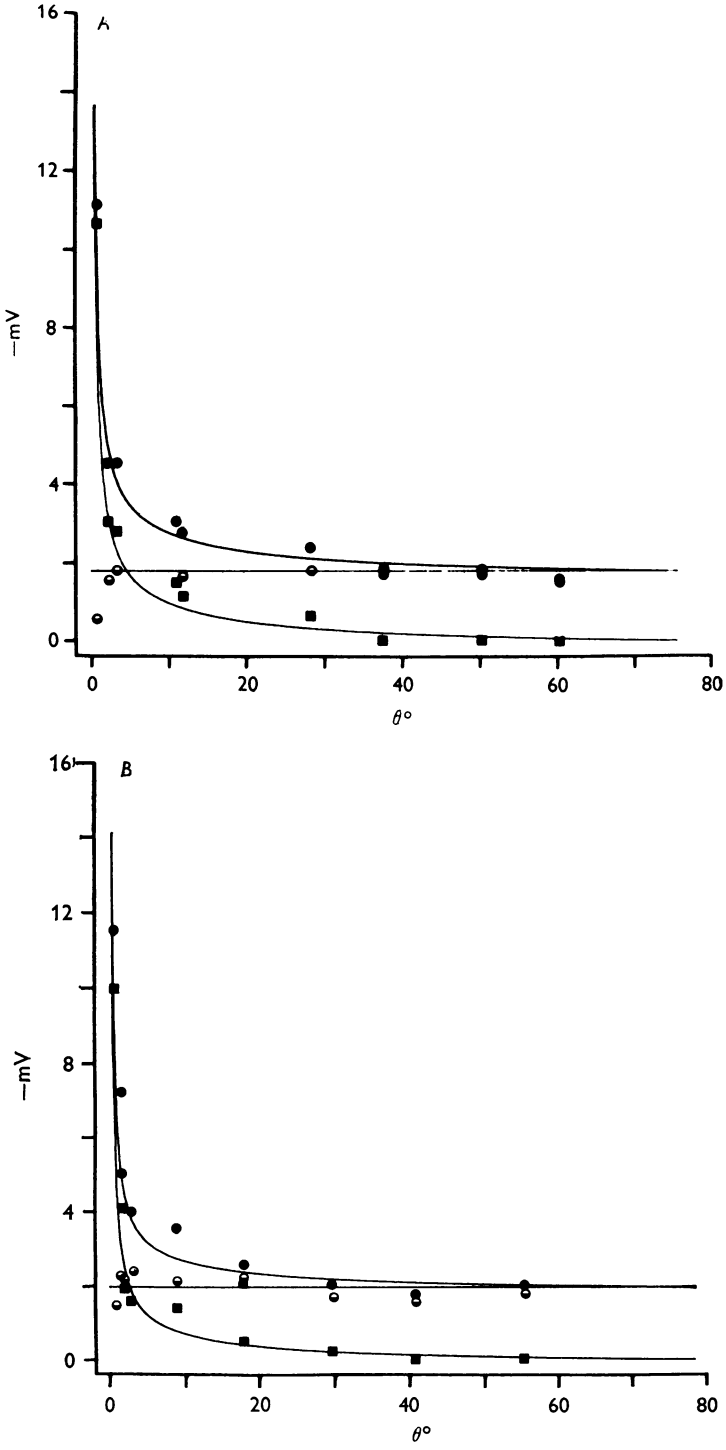

Fig. 5. For legend see facing page.

be appreciated that the basic predictions of the theoretical equation are supported. The total amplitude of the response decreases precipitously as electrode separation is increased, because the fast component steeply decrements while the slow component remains essentially constant.

If one plots the total amplitude of the induced potential in all twelve experiments against corresponding electrode angular separations (Fig. 6),

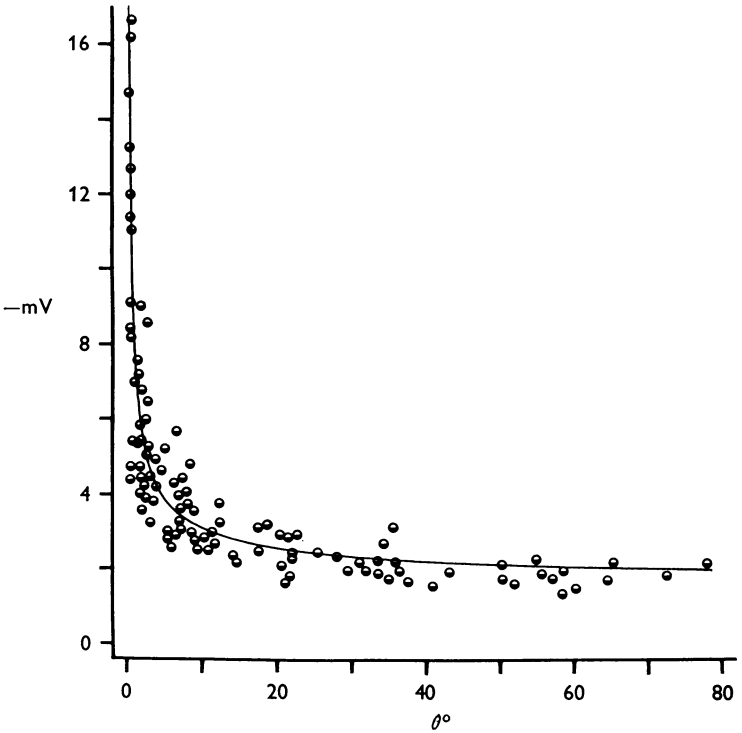

Fig. 6. Plot of total induced potential response as a function of electrode angular separations. Both electrodes are placed just under lens surface. Current pulses are 500 nA for 8 sec. Computer-drawn curve is calculated from eqn. (1) using R_i and R_m determined by applying curve fitting analysis to composite data. $R_m = 2751\ \Omega\ \text{cm}^2$ and $R_i = 625\ \Omega$ cm.

Fig. 5. Plots of induced potential as a function of angular separation for two typical experiments. Both electrodes are placed just under lens surface. Current pulses are 500 nA for 8 sec (total response) or 500 nA for 100 msec (fast component). ●, total response (b); ■, fast component (a); ◒, slow component ($b-a$). Computer drawn curves through total response points are calculated from eqn. (1) using R_m and R_i values determined from curve fitting analysis. Curves through fast component points are calculated from the last four terms of eqn. (1). Curves through slow component are calculated from the first term of eqn. (1).

it can be seen that the theoretical relationship correlates well with the composite data when $R_i = 625 \pm 49\ \Omega$ cm, and $R_m = 2751 \pm 165\ \Omega\ cm^2$ (best fit value $\pm$ asymptotic standard deviation) (Dixon, 1974). The best-fit values and variance for the parameters determined from the curve fitting programme for each of the twelve experiments are given in Table 1. Calculated by conventional formulae from these individual values, $R_i = 727 \pm 88\ \Omega$ cm and $R_m = 2645 \pm 102\ \Omega\ cm^2$. (Mean $\pm$ S.E. of mean.)

TABLE 1. Curve fitting from data of twelve experiments

Lens	R_i (Ω cm)	Asymptotic standard deviation of R_i	R_m ($\Omega\ cm^2$)	Asymptotic standard deviation of R_m	C_m ($\mu F/cm^2$)	r
FL1.ED	724	68	3060	213	—	0·996
FL2.ED	424	80	2657	352	—	0·989
FL3.ED	618	107	2404	213	—	0·997
FL4.ED	630	132	2537	328	—	0·989
FL5.ED	537	66	2482	245	278	0·993
FL6.ED	550	87	2931	315	246	0·991
FL7.ED	994	87	1906	217	514	0·997
FL8.ED	846	215	2777	684	345	0·980
FL9.ED	393	79	2725	344	234	0·989
FL10.ED	900	113	3288	269	237	0·998
FL12.ED	609	133	2509	556	199	0·992
FL13.ED	1499	83	2470	276	323	0·999

Because of the large increase in the induced voltage which occurs when the electrode tips are close together and because of the uncertainty in the measurement of the separation of the tips when they are close together, there is considerable scatter in those points. On occasion this scatter interfered with the curve fitting programme and so it was not consistently possible to obtain adequate curve fits for individual experiments when data for angular separations of $< 2°$ were included. However, the problem is purely a technical one (i.e. a defect in the curve fitting programme) because curves calculated from data with $> 2°$ angular separation did adequately fit the data for angular separations of $< 2°$. If all experiments were pooled, the R_m and R_i values calculated from angular separations $> 2°$ were 2805 $\Omega\ cm^2$ and 609 Ω cm respectively, whereas R_m and R_i values calculated from the data for all angular separations were 2751 $\Omega\ cm^2$ and 625 Ω cm respectively. On the plotter scales used in Fig. 6, the curves calculated from these parameter values were virtually identical. The goodness of fit coefficient is calculated as follows:

$$R = \left(1 - \frac{\text{mean square error}}{\text{variance of } y}\right)^{\frac{1}{2}} \quad \text{(Yule \& Kendall 1950).}$$

Membrane capacitances shown in the table were determined from single measurements in eight of the experiments for the relationship $C_m = TC/R_m$, where TC is the time for the voltage response to reach 63 % of its final displacement. For these experiments, $TC = 0{\cdot}758 \pm 0{\cdot}056$ sec (mean $\pm$ S.E. of mean). It can readily be seen that the value for R_m is comparable to those found in single cells, whereas both C_m and R_i are remarkably elevated (Katz, 1966).

The structure of the lens might lead one to expect severely anisotropic flow of current, at least if the distribution of tight junctions were as anisotropic as the distribution of the fibres which make up the lens. Four experiments were performed in which the potential was measured in many directions around a micro-electrode current source inserted just under the surface of the lens. The potential was essentially the same in every direction provided the potential was measured the same distance from the current electrode. On rare occasions, the potential at a single penetration was much larger than elsewhere. This would be expected if those rare occasions were when the current and voltage micro-electrodes were in the same fibre.

DISCUSSION

The data presented largely explain the discrepancies between the previous measurements of Duncan (1969) and those of Rae & Blankenship (1973). If the tips of the voltage and current electrodes had been 200 μm or more apart in Duncan's measurements, his records would have measured mostly the slow component which is independent of the separation of the electrodes. The fast component would have been difficult to identify. In the double-barrel measurements of Rae & Blankenship, the current and voltage electrode tips are as close together as possible. It is doubtful that in a two electrode experiment, the tips could ever be placed as close together. Consequently, the double-barrel technique must measure primarily the rapid component (local) potential. The slow component would not have been seen by Rae & Blankenship since with the 50 nA, 500 msec pulses used in that study, its amplitude would be expected to be only about 0·08 mV compared to the 50–300 mV size of the rapid component. Consequently, it seems reasonable that Duncan was measuring only the slow component, whereas Rae & Blankenship were measuring only the fast component. In the mapping technique reported in the present study, both components are measured in every lens.

Our present results verify the original observations of Duncan, that an induced potential can be measured in the lens for all separations of the current and internal voltage micro-electrodes. In almost every case one can be certain that the current micro-electrode and the internal voltage

micro-electrode are not in the same cell. Thus, the current injected into the cell containing the current micro-electrode induces a potential in another cell, the cell containing the voltage micro-electrode. Such a situation is usually described by saying the cells are electrically coupled.

Using our technique, it is only possible to estimate the degree of coupling. The amplitude of the rapid component of the induced potential depends entirely upon the internal resistivity and not at all upon membrane resistance, but the internal resistivity in turn depends upon both cytoplasmic resistivity and gap junctional resistivity R_j (Ω cm). Unfortunately, we cannot quantitatively separate R_i into its cytoplasmic and junctional components. It is, however, reasonable to assume that R_i depends primarily on gap junctional resistivity since (1) frog lens cells are only 59–60% water and thus their cytoplasm is a highly concentrated polyelectrolyte solution whose conductivity might be greater and not less than cells with a higher percentage of water; (2) our calculated R_i values of approximately 625 Ω cm are much larger than the cytoplasmic resistivity value of 130 Ω cm reported for the bovine lens cortex (Pauly & Schwann, 1964), and the 30–200 Ω cm cytoplasmic resistivity values reported for other cells (Katz, 1966). Therefore, the value of R_i that we get from our curve fitting analysis applied to each lens should give us a reasonable estimate of junctional resistivity. At the same time we obtain R_m which is a good measure of membrane resistance properties.

In order to convert our value of R_j, the specific resistivity of the junction to a membrane resistance R_{jm} (Ω cm^2), one must know S_j/V_l, the surface area of junctional membrane per unit volume of lens. We have no estimate of this junctional surface area at present.

The very high values of C_m obtained from our experiments suggests that we are not only charging the outer membranes of cells located at the surface of the lens, but must also be charging membranes of a significant number of cells located deep in the lens. The outer membranes would be expected to have a surface area of about 1 cm^2 in lenses of the size used for these experiments. If we assume that the lens membranes have the capacitance of 1–1·5 μF/cm^2 typical for other cells, then we must be charging 200–300 cm^2 of membrane surface in these studies and thus a large amount of cell membrane inside the lens. It is interesting that there seems to be little or no resistive current across the internal membranes, at least judging from the reasonable value of R_m.

Since we are able to measure both membrane resistance and junctional resistivity, we should be able to see if cataract formation in the crystalline lens is related to the functional integrity of cell-to-cell junctions. This hypothesis is an attractive one in light of data which suggests that intracellular Ca^{2+} increases in many forms of cataracts (Duncan, 1973). Such a

calcium increase might be expected to uncouple normally coupled cells (Loewenstein, 1966).

We thank Dr A. Peskoff for his critical reading of the manuscript and for most useful discussions based on a theoretical analysis of a model of the preparation.

This work was supported by research grants from the U.S.P.H.S. National Eye Institute (EY–01207) (Dr Rae) and National Science Foundation (GB–24965) (Dr Eisenberg).

REFERENCES

ANDREE, G. (1958). Über die natur des Transkapsularen Potentials Der linse. *Pflügers Arch. ges. Physiol.* **267**, 109–116.

Application Manual for Computing Amplifiers (1966). Philbrick Researches Inc., p. 66. New York: Nimrod Press Inc.

BARCILON, V., COLE, J. D. & EISENBERG, R. S. (1971). A singular perturbation analysis of induced electric fields in cells. *SIAM J. appl. Math.* **21**, 339–354.

BRINDLEY, G. S. (1956). Resting potential of the lens. *Br. J. Ophthal.* **40**, 385–391.

COHEN, A. I. (1965). The electron microscopy of the normal human lens. *Symposium on the Lens*, p. 57. St Louis: C. V. Mosby Co.

DIXON, W. J. (1974). Non-linear least squares in BMD biomedical computer programs. *Univ. Calif. Publs* **78**, 387.

DUNCAN, G. (1969). The site of the ion restricting membranes in the toad lens. *Expl Eye Res.* **8**, 406–412.

DUNCAN, G. (1973). Role of membranes in controlling ion and water movements in the human lens – in relation to cataract. *Ciba Fdn Symp. no.* 19. Amsterdam: ASP.

DUNCAN, G. & BUSHELL, A. R. (1975). Ion analyses of human cataractous lenses. *Expl Eye Res.* **20**, 223–230.

EISENBERG, R. S. & ENGEL, E. (1970). The spatial variation of membrane potential near a small source of current in a spherical cell. *J. gen. Physiol.* **55**, 736–757.

EISENBERG, R. S. & JOHNSON, E. A. (1970). Three-dimensional electrical field problems in physiology. *Prog. Biophys. molec. Biol.* **20**, 1–65.

KATZ, G. (1966). *Nerve, Muscle and Synapse*, pp. 46–47. New York: McGraw-Hill.

LOEWENSTEIN, W. R. (1966). Permeability of membrane junctions. *Ann. N.Y. Acad. Sci.* **137**, 441–472.

PAULY, H. & SCHWANN, H. P. (1964). The dielectric properties of the bovine eye lens. *IEEE Trans. bio-med. Engng* **11**, 103.

PESKOFF, A. & EISENBERG, R. S. (1973). Interpretation of some microelectrode measurements of electrical properties of cells. *A. Rev. Biophys. bioengng* **2**, 65–79.

PESKOFF, A. & EISENBERG, R. S. (1975). The time-dependent potential in a spherical cell using matched asymptotic expansions. *J. math. Biol.* **2**, 227–300.

RAE, J. L. (1973). The potential difference of the frog lens. *Expl Eye Res.* **19**, 235.

RAE, J. L. (1974*a*). Potential profiles in the crystalline lens of the frog. *Expl Eye Res.* **19**, 227.

RAE, J. L. (1974*b*). The movement of procion dye in the crystalline lens. *Invest. Ophthal.* **13**, 147.

RAE, J. L. & BLANKENSHIP, J. E. (1973). Bioelectric measurements in the frog lens. *Expl Eye Res.* **15**, 209.

RAFFERTY, N. S. & ESSON, E. A. (1974). An electron-microscope study of adult mouse lens: some ultrastructural specializations. *J. Ultrastruct. Res.* **46**, 239–253.

RAFFERTY, N. S. & GOOSSENS, W. (1975). Ultrastructural studies of traumatic cataractogenesis: observations of a repair process in mouse lens. *Am. J. Anat.* **142**, 177–199.

WANKO, T. & GAVIN, M. S. (1961). Cell surfaces in the crystalline lens. In *The Structure of the Eye*, ed. SMELSER, G. New York: Academic Press Inc.

YULE, G. U. & KENDALL, M. G. (1950). *An Introduction to the Theory of Statistics*, p. 361. New York: Hafner.